Mineralogical Magazine, February 1998, Vol. 62(1), pp. 41–54

Cation distribution in natural Zn-aluminate spinels

S. LUCCHESI

Dipartimento di Scienze della Terra, Università di Roma "La Sapienza", P. le A. Moro 5, 00186 Roma, Italy

A. DELLA GIUSTA

Dipartimento di Mineralogia e Petrologia, Università di Padova, Corso Garibaldi 37, 35122 Padova, Italy

AND

U. RUSSO

Dipartimento di Chimica Inorganica, Metallorganica e Analitica, Università di Padova, Via Loredan 4, 35131 Padova, Italy

ABSTRACT

The intracrystalline cation distributions in fourteen natural Zn-aluminate spinels were determined by means of X-ray single-crystal structural refinement, supported for some samples by Mössbauer spectroscopy.

Zinc substitutes for Mg and subordinately Fe^{2+} and its relevant changes in content, from 0.10 to 0.96 atoms per formula unit (apfu), are not related to variations of cell parameter. The latter is determined mainly by the substitution $Fe^{3+} \rightleftharpoons Al$. In agreement with data from synthetic samples, a small but definite amount of Zn (up to 0.06 apfu) is located in the octahedral M site. Fe^{2+}, when present, shows a preference for tetrahedral coordination.

An improved value of the tetrahedral Zn(T)–O distance (1.960 Å) was obtained, integrating the set of interatomic distances used for the determination of cation distribution in spinels.

KEYWORDS: spinel, zinc, gahnite, crystal chemistry, intracrystalline disorder.

Introduction

SPINELS are a class of ubiquitous and important rock-forming minerals, and their widespread occurrence has long suggested their use as petrogenetic indicators (e.g. Spry and Scott, 1986). A large number of investigations on intracrystalline disorder (Della Giusta *et al.*, 1996; Lucchesi and Della Giusta, 1997) on both natural and synthetic compounds has indicated their possible use for geothermometric purposes. In fact, in natural spinel crystals, the two cation sites available in the AB_2O_4 structure (*Fd3m* symmetry), one tetrahedral (T) site — $\bar{4}3m$ point symmetry — and one octahedral (M) — $\bar{3}m$ point symmetry — both with fixed coordinates (Hafner, 1960; Hill *et al.*, 1979), can be occupied by several cations, mainly divalent (A) and trivalent (B). Some of these cations, e.g. Mg, Al, Fe^{2+} and Fe^{3+}, under thermal treatment can exchange between the T and M sites in amounts as large as approximately 0.3 atoms (Wu and Mason, 1981; Wood *et al.*, 1986; O'Neill, 1992; Roelofsen *et al.*, 1992). The disordered configuration relations between the tetrahedral and octahedral sites of the A and B cations may thus be described by an inversion parameter i:

$$^{IV}(A_{1-i}B_i)^{VI}(B_{2-i}A_i)O_4$$

Normal spinels are those with i = 0, inverse those with i = 1, as magnetite. While a large quantity of data is presently available for simple binary spinels, both concerning their cation distribution and its temperature dependence

(e.g. O'Neill, 1992; Wu and Mason, 1981; O'Neill *et al.*, 1992), far less work has been done on multicomponent spinel solid-solutions (Nell *et al.*, 1989; Larsson, 1995) and the precision of these investigations is, at times, poorly known.

Complete knowledge of cation distribution is thus fundamental for a full understanding of spinel properties. This knowledge may be obtained by the precise characterization of octahedral and tetrahedral site preferences of the constituent cations, in both normal and inverse configurations.

Topochemical relations in natural spinels may be determined by combining the information from single-crystal X-ray diffraction and very accurate microprobe analyses. In this method, each cation is characterized by its site bond-distance and valency status; thus, the availability of an accurate and self-consistent set of distances is essential. Improvements to the ionic radii proposed by Shannon (1976) have been developed for spinels by several authors (e.g. O'Neill and Navrotsky, 1983; Marshall and Dollase, 1984). In previous papers (Della Giusta *et al.*, 1996; Lucchesi *et al.*, 1997), an improved and self-consistent set of bond-distances was obtained, for octahedral and tetrahedral coordination, for the commonest cations in natural spinels (Mg, Al, Fe^{2+}, Fe^{3+}, Mn, Cr). These data were used to calculate the cation intracrystalline distribution in a pleonaste crystal from volcanic ejecta which turned out to be highly disordered (Lucchesi and Della Giusta, 1997).

This paper presents the results of microprobe analyses and single-crystal X-ray structural refinements of 14 natural aluminate spinels with the general formula $Zn_x(Mg,Fe^{2+})_{1-x}(Al,Fe^{3+})_2O_4$, where $0.08 \leqslant x \leqslant 0.96$. Other cations occur only in minor amounts. The aim was to investigate the effects of the presence of a cation like Zn, with a relatively high preference for tetrahedral coordination (O'Neill and Navrotsky, 1983; Navrotsky, 1986), on the intracrystalline distribution of the remaining cations. The samples were chosen so as to contain the lowest possible quantity of Mn^{2+}: in fact, with the adopted method, the presence of this element, which in large quantities may disorder into the M site (Lucchesi *et al.*, 1997), would hide the expected low amounts of octahedral Zn. Further studies will be devoted to the crystal chemistry of Zn in ferrites (franklinite) and in the haeterolite–hausmannite binary.

Zinc crystal chemistry in *Fd3m* aluminates

Zn-aluminates are generally assumed to be essentially normal spinels (Navrotsky, 1986) because of the excess energy stabilization of the zinc ion in the tetrahedral coordination, due to its tendency to form sp^3 covalent bonds (O'Neill and Navrotsky, 1983). However, energy calculations have led most authors to predict the existence of a very minor inversion in $Zn(Al, Fe)_2O_4$ (Spry and Scott, 1986) and even in $Zn(Al, Cr)_2O_4$ (Bruckmann-Benke *et al.*, 1988), in which the high octahedral site-preference of Cr further hinders the inversion process, as experimentally noted by O'Neill and Dollase (1994) on synthetic $ZnCr_2O_4$, a totally normal spinel. Neutron diffraction experiments (Fischer, 1967) did not allow unambiguous direct observation of zinc intracrystalline disorder, since a synthetic Zn-aluminate with a = 8.086(1) Å and oxygen coordinate u = 0.2636(1) had i = 0.03(3), a value within the limits of experimental uncertainty. However, the presence of a very minor amount of inversion was experimentally verified in a synthetic Zn-aluminate by Cooley and Reed (1972) after it was annealed at high temperatures (i = 0.04 at 905°C and i = 0.06 at 1197°C) and O'Neill and Dollase (1994), who observed small departures from completely normal cation distribution (from i = 0.011(7) at 900°C to i = 0.053(6) at 1300°C). Both papers highlighted the usual tendency of ordering with progressive decrease of annealing temperature.

In the presence of iron, the Zn behaviour seems to depend on the different iron oxidation states. In synthetic $Zn(Al, Fe)_2O_4$ spinels, the tendency of zinc towards intracrystalline disorder, recognized in synthetic Zn-ferrites (O'Neill, 1992), has been observed (Waerenborgh *et al.*, 1994b). In the latter paper, zinc was unambiguously assigned to octahedral sites (i = 0.02 for $Zn(Al_{1.9}Fe_{0.1})O_4$ and i = 0.05 for $Zn(Al_{1.4}Fe_{0.6})O_4$, both at 727°C), the Fe^{3+} fraction in tetrahedral sites being larger than the Al(T) one. An increase in annealing temperature to 1077°C resulted in the usual increase in inversion (i = 0.04 and 0.08 respectively). However, the same authors (Waerenborgh *et al.*, 1994*a*) could not positively show the existence of octahedral zinc in $(Zn, Fe)Al_2O_4$ synthetic crystals, which were thus considered as totally normal, with only one case of 0.009 Zn(M) apfu. In these crystals, minor amounts of Fe^{3+} due to partial iron oxidation were noted, and their disordering in tetrahedral coordination was considered to be

responsible for possible, although highly improbable, zinc inversion.

Studies on natural samples are comparatively less abundant and more contradictory. An X-ray investigation (Saalfeld, 1964) on a gahnite crystal from Falun, Sweden, showed a totally normal character with a = 8.099(2) Å and T–O = 1.88 Å and M–O = 1.96 Å, notwithstanding the presence of large amounts of Fe and Mg in both T and M sites. Mössbauer investigations (Waerenborgh *et al.*, 1990) on three natural gahnites and kreittonites suggested totally ordered iron distribution with Fe^{2+} in tetrahedral sites and Fe^{3+} in octahedral ones.

Experimental

The examined samples (Table 1) constitute a set of 14 crystals in the gahnite–spinel (*s.s.*)–hercynite system, kindly made available by the Museum of Mineralogy, University of Rome "La Sapienza", Italy.

Small equidimensional fragments of the selected crystals were mounted, for X-ray data collection, on a Siemens P4 automated four-circle, single-crystal diffractometer. Details of data collection are shown in Table 2, and further information may be found in Lucchesi *et al.* (1997).

No significant deviations from *Fd*3*m* symmetry were noted: the appearance of forbidden space-group reflections such as 200 was attributed, on the basis of Psi-scan checks, to double reflection (Tokonami and Horiuchi, 1980). The oxygen coordinate, M and T occupancies, secondary extinction coefficient, scale factor and thermal factors were the variable parameters. The starting oxygen coordinate was that proposed by Princivalle *et al.* (1989), setting the origin at $\bar{3}$m. Isotropic secondary extinction was corrected according to Larson's (1970) algorithm. No chemical constraints were used during refinement. Fully ionized scattering curves for all elements except oxygen (20% ionized) were used, since they proved to furnish the best values of conventional agreement factors over all $\sin\theta/\lambda$ intervals and the best coherence between observed and calculated F(222), the latter structure factor being particularly sensitive to M and O site occupancies (Della Giusta *et al.*, 1986). Off-diagonal thermal factors were extremely small and of the same magnitude as their σ, when not forced by symmetry to zero values, and thus only U_{11} values are shown in Table 3. Three isotropic, full-matrix, refinement cycles were followed by anisotropic cycles until convergence was attained. The disagreement coefficient (R) values were very satisfactory (Table 3).

The same crystals used for X-ray data collection were mounted on a glass slide and polished for electron microprobe analysis (WDS method) on a Cameca-Camebax instrument with the PAP data reduction program. Synthetic oxide standards (MgO, FeO, MnO, ZnO, NiO, CuO, Al_2O_3, Cr_2O_3, V_2O_3, TiO_2, SiO_2) were used (see Lucchesi *et al.* (1997) for details of instrument

TABLE 1. Description and provenance of natural Zn-aluminate spinels

Sample	Variety	Provenance	Reference #	Colour
SPN 112	Gahnite	Falun, Sweden	2988/112	Dark green
SPN 115a	Dysluite	New York, USA	2991/115	Blue
SPN 115b	Dysluite	New York, USA	2991/115	Light green
SPN 116	Dysluite	Sterling, N.J., USA	2992/116	Honey yellow
SPN 117	Dysluite	Franklin, N.J., USA	2993/117	Dark green
SPN 118	Dysluite	Franklin, N.J., USA	2994/118	Honey yellow
SPN 127	Gahnite	Falun, Sweden	5171/127	Dark green
SPN 190	Zn-Spinel	Tiriolo, Calabria, Italy	13747/190	Blue-green
SPN 193	Zn-Spinel	Tiriolo, Calabria, Italy	13958/193	Blue-green
SPN 228	Kreittonite	Bodenmais, Bavaria, Germany	18820/228	Black
SPN 230	Dysluite	Sterling, N.J., USA	19970/230	Black-green
SPN 232	Kreittonite	Bodenmais, Bavaria, Germany	20822/232	Blue-green
SPN 244	Gahnite	Charlemont, Mass., USA	22759/244	Black-green
SPN 249	Zn-Spinel	Tiriolo, Calabria, Italy	23838/249	Blue-green

TABLE 2. Parameters for X-ray data collection

Unit cell parameter determination:	
Radiation (Å)	Mo-$K\alpha_1$ (0.70930)
Reflections used	12 (Friedel pairs on both +2θ and −2θ)
Range (2θ)	83°−92°
Temperature (K)	296
Diffraction intensity collection:	
Radiation (Å)	Mo-$K\alpha$ (0.71073)
Monochromator	High crystallinity graphite crystal
Range (2θ)	3°−95°
Reciprocal space range	$0 \leqslant h,k,l \leqslant 17$
Scan method	Omega
Scan range (2θ)	2.4°
Scan speed (2θ/min)	Variable 2.93°−29.3°
Temperature (K)	296
Data reduction:	
Refinement	SHELXTL
Corrections	Lorentz, Polarization
Absorption correction	Semi-empirical, 13 psi scans (0°−95° 2θ)
Set of observed reflections	707−717 ($I > 2\sigma$)
Set of unique reflections	147−149

calibration). Precision for major elements (Mg, Al, Fe) was usually within 1% of the actual amount present, while that of minor elements was within about 5%. Contents of Fe^{3+} were calculated on the basis of stoichiometry: 3 cations for 4 oxygen atoms. Standard deviations of cations were calculated according to Wood and Virgo (1989). The elements Ni, Cu, V and Si were not observed. Results are shown in Table 4. Very great care was devoted to the microprobe analyses — no less than 15 point analyses were performed on each sample — since only two samples, SPN116 and SPN118, were available in sufficient amounts for Mössbauer verification of the Fe^{2+}/Fe^{3+} ratio.

The samples for Mössbauer measurements were prepared by finely grinding 16 mg of each spinel in an agate mortar under acetone. The powder was then suspended in vaseline and wrapped in thin plastic foil. Spectra were obtained in a conventional constant acceleration spectrometer using a rhodium matrix ^{57}Co source (nominal strength 50 mCi) kept at room temperature; the spectrometer was calibrated at room temperature with α-iron foil. Mirror symmetric spectra were accumulated in a 512 channel analyser, folded, and fitted to pure Lorentzian line-shapes with the aid of a least-squares fitting program.

Results

Cation distribution

The cation distribution of the investigated Zn-spinels is rather complex, involving five cations (Al, Zn, Mg, Fe^{2+}, Fe^{3+}) that may be distributed on both T and M sites.

Intracrystalline distribution was obtained by a minimization program which takes into account both structural and chemical data (Carbonin *et al.*, 1996). The minimized function is:

$$f(X_i) = \sum_{j=1}^{n} \left(\frac{O_j - C_j(X_i)}{\sigma_j} \right)^2$$

where O_j is the observed quantity, σ_j its standard deviation and C_j the same quantity calculated by means of X_i parameters. The n C_j quantities were: a, u, the site electrons e^-(T) and e^-(M), the number of atoms per formula unit (3) and the number in T and M sites (1 and 2 respectively), the number of charges for balance and the total atomic proportions from microprobe analyses. The X_i parameters were the cation fractions in both sites.

The a and u values depend on the T-O and M−O site bond distances (Hafner, 1960; Hill *et al.*, 1979) and are thus linked to the cation site

TABLE 3. Crystal data and results of structural refinement

Sample	Dimensions[a]	a[b]	u	T–O[b]	M–O[b]	occ.(T)[c]	occ.(M)[c]	U_{11} (T,M,O)[d]			ext.	R[e]	N[e]
SPN 112	0.19 × 0.18 × 0.20	8.0946(2)	0.26406(6)	1.9497(8)	1.9166(4)	26.40(9)	12.95(5)	74(1)	60(2)	69(2)	0.0080(5)	1.79	147
SPN 115a	0.21 × 0.19 × 0.23	8.1041(3)	0.26419(6)	1.9538(8)	1.9179(4)	27.43(9)	13.06(4)	57(1)	45(2)	55(2)	0.0050(4)	1.53	147
SPN 115b	0.19 × 0.13 × 0.10	8.1197(3)	0.26405(7)	1.9556(10)	1.9226(5)	29.50(11)	14.19(6)	36(1)	34(2)	40(2)	0.0017(2)	1.90	149
SPN 116	0.17 × 0.24 × 0.28	8.1443(3)	0.26359(7)	1.9550(10)	1.9317(5)	29.71(16)	14.81(9)	82(1)	75(2)	89(2)	0.0034(3)	2.10	149
SPN 117	0.19 × 0.21 × 0.28	8.1191(2)	0.26386(6)	1.9527(8)	1.9238(4)	29.53(11)	13.90(4)	72(1)	61(2)	74(2)	0.0041(3)	1.78	149
SPN 118	0.17 × 0.20 × 0.21	8.1328(3)	0.26371(8)	1.9539(11)	1.9282(6)	29.47(15)	14.40(8)	72(1)	65(2)	80(2)	0.0036(3)	1.89	149
SPN 127	0.17 × 0.19 × 0.32	8.0954(2)	0.26381(8)	1.9463(11)	1.9186(6)	26.43(13)	12.98(7)	78(2)	59(2)	68(2)	0.0064(7)	2.18	147
SPN 190	0.21 × 0.22 × 0.26	8.0970(2)	0.26372(5)	1.9455(7)	1.9196(4)	14.55(7)	13.01(5)	45(2)	31(2)	44(2)	0.0141(11)	2.08	147
SPN 193	0.18 × 0.17 × 0.12	8.0943(3)	0.26370(5)	1.9445(7)	1.9191(4)	15.76(8)	12.91(5)	70(2)	56(1)	70(2)	0.0090(7)	2.08	147
SPN 228	0.16 × 0.19 × 0.23	8.1196(2)	0.26436(7)	1.9599(10)	1.9204(5)	27.40(53)	13.40(5)	92(1)	79(2)	90(2)	0.044(2)	2.10	149
SPN 230	0.22 × 0.21 × 0.26	8.1218(2)	0.26378(10)	1.9523(14)	1.9250(7)	29.36(16)	13.82(6)	76(1)	63(2)	78(3)	0.0019(3)	2.21	149
SPN 232	0.18 × 0.21 × 0.12	8.1081(3)	0.26413(6)	1.9539(8)	1.9193(4)	27.76(17)	13.18(4)	61(1)	50(2)	62(2)	0.0018(2)	1.73	147
SPN 244	0.23 × 0.21 × 0.26	8.0982(3)	0.26394(8)	1.9488(11)	1.9183(6)	29.10(27)	12.99(7)	75(2)	57(2)	65(3)	0.0059(8)	2.31	147
SPN 249	0.18 × 0.19 × 0.21	8.0949(3)	0.26363(6)	1.9437(8)	1.9197(4)	14.66(8)	12.87(6)	78(2)	62(2)	76(2)	0.0046(6)	2.05	147

u: Oxygen coordinate; ext.: Isotropic secondary extinction coefficient; R: Disagreement coefficient; N: Number of independent observed reflections.
[a] Dimensions (mm); [b] Cell parameter and bond distances (Å); [c] Site occupancies (e^-); [d] Thermal factors ($Å^2 \times 10^4$); [e] Only reflections with $I > 2\sigma$ (I).

TABLE 4. Electron microprobe analyses of Zn-aluminate natural spinels

Sample	MgO	ZnO	MnO	FeO	Al_2O_3	Fe_2O_3*	Cr_2O_3	Total
SPN 112	3.91	35.09	0.12	3.87	56.76	–	–	99.83
SPN 115a	1.80	33.71	0.68	6.47	55.85	1.76	tr.	100.35
SPN 115b	0.49	41.89	0.72	–	49.35	8.27	0.13	100.93
SPN 116	0.45	41.56	0.51	–	45.13	13.26	tr.	101.57
SPN 117	0.48	42.00	0.60	0.14	50.00	7.52	tr.	100.89
SPN 118	0.37	40.76	0.80	0.39	46.74	10.22	0.17	99.60
SPN 127	4.35	34.28	0.13	2.99	57.43	1.33	–	100.60
SPN 190	23.48	4.33	0.37	2.31	67.17	2.38	–	100.11
SPN 193	21.43	9.09	0.30	1.30	66.47	2.15	–	100.77
SPN 228	2.43	28.73	0.41	9.97	54.30	4.03	–	99.94
SPN 230	0.84	40.44	0.89	0.57	49.47	8.47	0.06	100.85
SPN 232	1.63	33.09	0.41	7.01	54.03	3.10	tr.	99.34
SPN 244	1.47	38.15	0.08	3.22	54.98	1.95	–	99.93
SPN 249	23.14	5.96	0.45	1.51	67.29	2.25	–	100.62

Cations (4 oxygens) Sample	Mg	Zn	Mn	Fe^{2+}	Al	Fe^{3+}	Cr	Total
SPN 112	0.172(2)	0.762(7)	0.003(1)	0.063(3)	1.968(7)	0.032(6)	–	3.000
SPN 115a	0.080(3)	0.742(8)	0.017(2)	0.161(5)	1.961(10)	0.039(8)	–	3.000
SPN 115b	0.023(2)	0.959(8)	0.019(2)	0.000	1.803(9)	0.193(6)	0.003(1)	3.000
SPN 116	0.021(1)	0.965(10)	0.027(2)	0.000	1.673(10)	0.314(9)	–	3.000
SPN 117	0.022(1)	0.960(13)	0.016(3)	0.002(18)	1.823(17)	0.177(16)	–	3.000
SPN 118**	0.018(2)	0.954(11)	0.021(2)	0.008(5)	1.747(11)	0.246(9)	0.004(1)	3.000
SPN 127	0.189(6)	0.737(10)	0.003(1)	0.071(3)	1.970(10)	0.030(9)	–	3.000
SPN 190	0.865(3)	0.079(3)	0.008(1)	0.048(1)	1.956(4)	0.044(3)	–	3.000
SPN 193	0.799(3)	0.168(4)	0.006(1)	0.026(3)	1.959(5)	0.041(4)	–	3.000
SPN 228	0.108(3)	0.633(5)	0.011(1)	0.248(5)	1.909(7)	0.091(6)	–	3.000
SPN 230	0.039(1)	0.923(11)	0.023(2)	0.015(16)	1.802(14)	0.197(14)	0.002(1)	3.000
SPN 232	0.073(2)	0.740(8)	0.011(1)	0.176(6)	1.928(9)	0.072(8)	–	3.000
SPN 244	0.066(1)	0.850(9)	0.002(1)	0.081(9)	1.956(11)	0.044(10)	–	3.000
SPN 249	0.852(29)	0.109(23)	0.009(4)	0.030(3)	1.958(30)	0.043(27)	–	3.000

* Calculated.
** SPN118 also contains Ti 0.002(1) apfu.

fractions (X_i) according to:

$$T-O = \Sigma_i X_{T,i}(T-O)_i$$

and

$$M-O = \Sigma_i X_{M,i}(M-O)_i$$

where $X_{T,i}$ and $X_{M,i}$ are the cation site-fractions in tetrahedral (T) and octahedral (M) coordination and $(T-O)_i$ and $(M-O)_i$ the corresponding 'ideal' bond distances. The $(T-O)_i$ and $(M-O)_i$ set used in the minimization is that proposed by Della Giusta *et al.* (1996), integrated with the $Mn^{2+}(T)-O$ distance (Lucchesi *et al.*, 1997).

Site electronic densities $e^-(T)$ and $e^-(M)$ were calculated according to: $e^-(T) = \Sigma_i X_{T,i} Z_i$ and $e^-(M) = \Sigma_i X_{M,i} Z_i$, that is, as a linear contribution of the atomic number (Z_i) of each cation and its site molar fraction (X_i).

The following assumptions were made at the beginning of the minimization: (*a*) Zn, Mg, Al, Fe^{2+} and Fe^{3+} are equally distributed in both T and M sites; (*b*) on the basis of their general site preference, the small amounts of Cr and Ti are fixed in the M site (Marshall and Dollase, 1984; O'Neill and Dollase, 1994; Della Giusta *et al.*, 1996) and Mn^{2+} in the T site (Lucchesi *et al.*, 1997); (*c*) the sum (in T + M sites) of the cation fractions need not be equal to the microprobe value; (*d*) no constraints are fixed for maxima and minima.

As already noted, the site occupancies of these spinels are strongly dependent on the ionization level of the adopted scattering curves. However, while the total number of electrons e^-(tot.) may change by up to 1 e^-, the e^-(T)/e^-(M) ratio remains unchanged. This is most probably a consequence of the isotropic extinction factor in the adopted refinement program, since measurements of the intensities of the equivalent reflections often showed anisotropic extinction. The experience of our laboratories is that differences between the total number of electrons from the accurately calibrated microprobe and those from site occupancies are always lower than 0.5%. Consequently, the e^-(T) and e^-(M) values were rescaled to the microprobe e^-(tot.), in order to avoid overestimation of this factor in the minimization.

Results showed a systematic increase in minimization residuals with Zn content. This suggested that the Zn^{2+}(T)–O bond distance should be changed, repeating the minimization of all samples. The Zn^{2+}(T)–O bond distance was changed by 0.0005 Å at a time, and the best result was obtained at a value of 1.960 Å, i.e. slightly lower than that of Mg^{2+} (Mg(T)–O = 1.996 Å, Della Giusta *et al.*, 1996).

We used this method since data from synthetic Zn spinels show great differences according to composition. For instance, Zn(T)–O turns out to be 1.953 Å in $ZnAl_2O_4$ and 1.967 Å in $ZnCr_2O_4$ (O'Neill and Dollase, 1994) and 1.984 Å in $ZnFe_2O_4$ (O'Neill, 1992). Similar differences — up to 0.030 Å, more than ten times the experimental sigmas — are also shown by other cations. A consequence of this is that it is impossible to obtain a single set of bond distances which satisfactorily fits the geometric parameters of synthetic spinels. Instead, this is possible for natural spinels, as well as for other minerals such as olivine, garnet, clino- and orthopyroxene. Ample literature about the use of bond distances to determine the cation distribution of these minerals for petrological purposes exists, and testifies that bond distances are approximately constant — with an uncertainty of some digits to the third decimal point — at least within each class of compounds.

Intracrystalline distributions are reported in Table 5. Table 6 shows the minimization data compared with the observed data. The atomic fractions in Table 5 are shown to the fourth decimal point, only to allow comparison with the calculated data collected in Table 6. Correct evaluation of the standard deviation of the atomic fractions in each site is not simple, but we may assume a value about twice that calculated in Table 4 as a sufficient estimate.

Crystal chemistry

The aluminate spinels investigated here cover a relatively wide compositional range (Table 4) and contain, besides Mg, Al and Zn, relevant amounts of Fe^{2+} (up to *c.* 0.25 apfu in SPN228 and SPN232, both samples being of the kreittonite variety) and Fe^{3+}, up to 0.31 apfu. The elements Al and Fe^{3+} are the only important trivalent cations. Minor amounts of Mn^{2+} and Cr are also present. Of the divalent cations, the main substitution is Zn for Mg (Fig. 1) and Fe^{2+}, the latter mainly in the kreittonites. Progressive enrichment in zinc does not determine variations in *a*. Considering samples from the same locality, it is apparent that *a* may decrease with increasing Zn content (Tiriolo, Silberberg, Falun), remain unchanged (Franklin, Sterling), or even increase (New York) (Table 3). Instead, cell parameter variations are essentially determined by the substitution $Fe^{3+} \rightleftharpoons Al^{3+}$ (Fig. 2). The small quantities of Mn^{2+} (except in SPN228) generally increase with Fe^{3+}.

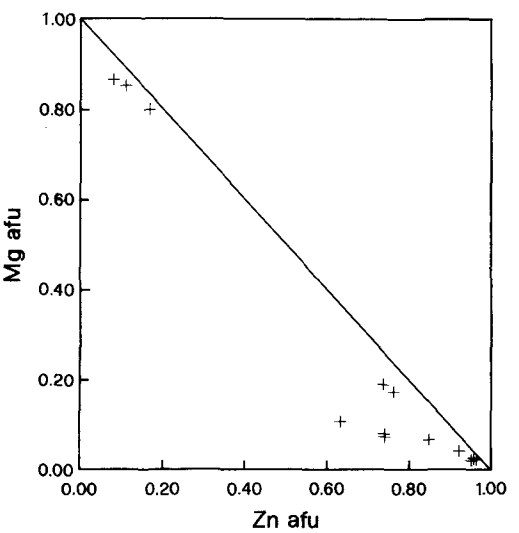

FIG. 1. Natural Zn-aluminates: Mg *vs* Zn content variations. Scatter of points to the left of the line representing the Mg $\rightleftharpoons$ Zn substitution is due to (Mn^{2+} + Fe^{2+}) $\rightleftharpoons$ Zn substitution.

TABLE 5. Cation distribution of natural Zn-aluminate spinels, as obtained from the minimization procedure

Sample	Site	Mn	Fe^{2+}	Zn	Mg	Al	Fe^{3+}	Cr	Total
SPN 112	T	0.0029	0.0631	0.7529	0.1038	0.0606	0.0165	–	0.9997
	M	–	0.0001	0.0081	0.0675	1.9085	0.0155	0.0000	1.9997
SPN 115a	T	0.0173	0.1465	0.7204	0.0236	0.0530	0.0391	–	1.0000
	M	–	0.0148	0.0212	0.0561	1.9079	0.0000	0.0000	2.0000
SPN 115b	T	0.0187	0.0000	0.9118	0.0000	0.0049	0.0643	–	0.9998
	M	–	0.0000	0.0457	0.0227	1.7998	0.1286	0.0031	1.9999
SPN 116	T	0.0269	0.0000	0.9017	0.0000	0.0028	0.0679	–	0.9993
	M	–	0.0000	0.0541	0.0209	1.6795	0.2472	0.0000	2.0017
SPN 117	T	0.0156	0.0000	0.9312	0.0000	0.0000	0.0510	–	0.9979
	M	–	0.0021	0.0289	0.0229	1.8243	0.1244	0.0000	2.0026
SPN 118	T	0.0214	0.0000	0.8967	0.0000	0.0000	0.0811	–	0.9992
	M*	–	0.0083	0.0588	0.0180	1.7468	0.1636	0.0040	2.0013
SPN 127	T	0.0031	0.0715	0.7298	0.0943	0.0779	0.0233	–	0.9998
	M	–	0.0000	0.0063	0.0941	1.8924	0.0071	0.0000	1.9998
SPN 190	T	0.0077	0.0479	0.0761	0.7505	0.0894	0.0277	–	0.9993
	M	–	0.0001	0.0028	0.1103	1.8701	0.0159	0.0000	1.9992
SPN 193	T	0.0063	0.0264	0.1673	0.6853	0.0877	0.0262	–	0.9992
	M	–	0.0000	0.0002	0.1093	1.8747	0.0148	0.0000	1.9991
SPN 228	T	0.0106	0.2285	0.6349	0.0434	0.0367	0.0464	–	1.0005
	M	–	0.0206	0.0001	0.0649	1.8702	0.0447	0.0000	2.0005
SPN 230	T	0.0233	0.0000	0.8887	0.0000	0.0001	0.0867	–	0.9987
	M	–	0.0150	0.0329	0.0393	1.8046	0.1090	0.0001	2.0010
SPN 232	T	0.0105	0.1649	0.7369	0.0050	0.0561	0.0266	–	0.9999
	M	–	0.0112	0.0026	0.0684	1.8721	0.0456	0.0000	1.9999
SPN 244	T	0.0021	0.0651	0.8494	0.0000	0.0380	0.0441	–	0.9986
	M	–	0.0161	0.0000	0.0664	1.9186	0.0000	0.0000	2.0010
SPN 249	T	0.0093	0.0301	0.1084	0.7335	0.0962	0.0216	–	0.9992
	M	–	0.0000	0.0000	0.1133	1.8652	0.0206	0.0000	1.9990

Atomic frequencies are given to the fourth decimal point for calculation purposes only. For an estimate of the uncertainty, refer to standard deviations of Table 4.
* Contains Ti 0.0018.

The T–O bond distance ranges from 1.944 Å to 1.960 Å, due to the substitution (Zn + Mg) for Fe^{2+} (Table 5). These T–O values, as a consequence of the fact that the values of Zn and Mg tetrahedral bond-distances are similar, are not related to the variations in Zn content with progressive Mg substitution. Instead, ferrous iron, which is mainly ordered in the tetrahedral site (Fe^{2+}(T)–O = 1.996 Å), when present in significant amounts, causes an increase in the T–O values (Fig. 3). In contrast, given their short site bond-distances (Al(T)–O = 1.767 Å and Fe^{3+}(T)–O = 1.891 Å), even small amounts of Al(T) + Fe^{3+}(T) result in a contraction of the T–O values. The electronic density of the T site is highly variable, ranging from 14.7 e^- (SPN249) to about 29.7 e^- (SPN116), essentially because of the amply variable Zn(T) site contents. Despite the recognized tendency of Mn^{2+} towards intracrystalline disorder in galaxite and jacobsite (Lucchesi *et al.*, 1997), this cation was fixed in the T site due to its low content (less than 0.03 apfu), since significant amounts of Mn^{2+} are known to occupy octahedral sites significantly only in crystals with total Mn content higher than 0.2 apfu (Lucchesi *et al.*, 1997).

In all samples the octahedral bond-distance is shorter than the tetrahedral one, as a consequence of the oxygen fractional coordinate, which is higher than 0.2625 (for this value T–O = M–O; Hill *et al.*, 1976). Such a short M–O bond distance, from 1.917 Å to 1.932 Å, is a direct consequence of the large amounts of Al and of its general preference for the M site (Fig. 4).

TABLE 6. Observed and calculated structural parameters of natural Zn-aluminate spinels

Sample	*a*		u		e^-(T)		e^-(M)	
	obs.	calc.	obs.	calc.	obs.	calc.	obs.	calc.
SPN 112	8.0946(2)	8.0946	0.26406(6)	0.26406	26.40(9)	26.76	12.95(5)	13.13
SPN 115a	8.1041(3)	8.1041	0.26419(6)	0.26419	27.43(9)	27.84	13.06(4)	13.25
SPN 115b	8.1197(3)	8.1197	0.26405(7)	0.26405	29.50(11)	29.56	14.19(6)	14.23
SPN 116	8.1443(3)	8.1444	0.26359(7)	0.26363	29.71(16)	29.53	14.81(9)	15.07
SPN 117	8.1191(2)	8.1191	0.26386(6)	0.26391	29.53(11)	29.65	13.90(4)	14.07
SPN 118	8.1328(3)	8.1328	0.26371(8)	0.26375	29.47(15)	29.55	14.40(8)	14.65
SPN 127	8.0954(2)	8.0954	0.26381(8)	0.26381	26.43(13)	26.58	12.98(7)	13.05
SPN 190	8.0970(2)	8.0970	0.26372(5)	0.26372	14.55(7)	14.61	13.01(5)	13.07
SPN 193	8.0943(3)	8.0944	0.26370(5)	0.26370	15.76(8)	15.91	12.91(5)	13.04
SPN 228	8.1196(2)	8.1196	0.26436(7)	0.26436	27.40(53)	27.46	13.40(5)	13.40
SPN 230	8.1218(2)	8.1218	0.26378(10)	0.26385	29.36(16)	29.50	13.82(6)	14.07
SPN 232	8.1081(3)	8.1081	0.26413(6)	0.26413	27.76(17)	28.14	13.18(4)	13.36
SPN 244	8.0982(3)	8.0982	0.26394(8)	0.26398	29.10(27)	28.87	12.99(7)	13.08
SPN 249	8.0949(3)	8.0951	0.26363(6)	0.26363	14.66(8)	14.88	12.87(6)	13.07

u: Oxygen coordinate. Cell parameter (Å); site occupancies (e^-).

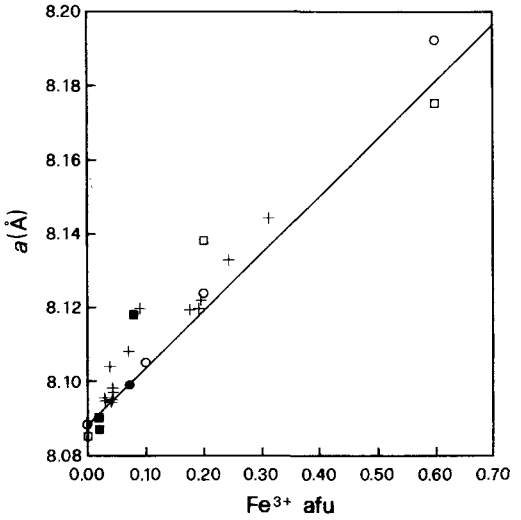

FIG. 2. Natural Zn-aluminates: a *vs* Fe^{3+} content variations. Crosses: data from the present work; Full squares: natural samples (Waerenborgh *et al.*, 1990); Full circle: natural sample (Saalfeld, 1964); Open squares: synthetic $Zn(Al, Fe)_2O_4$ (Carvalho and Sclar, 1988); Open circles: synthetic $Zn(Al, Fe)_2O_4$ (Waerenborgh *et al.*, 1994*a*). Line shows the calculated values for $Zn(Al, Fe)_2O_4$ cubic spinels as obtained from the bond distances used in this paper. All natural data lie above this line because of the substitution of Zn by other bivalent cations. Synthetic data from literature, relative to nominal compositions Fe^{3+} 0.2 and 0.6, show a remarkable scatter presumably due to poor chemical characterization. Literature data concerning synthetic $ZnAl_2O_4$ end-member are all very close to 8.088 Å (see text).

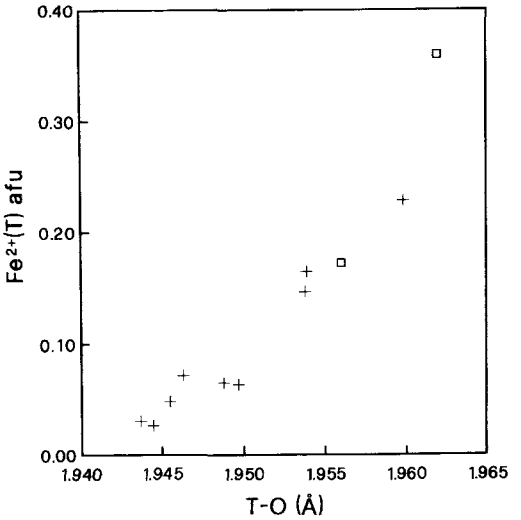

FIG. 3. Natural Zn-aluminates: Fe^{2+}(T) content variations *vs* T-O bond distance. Crosses: data from the present work; Open squares: synthetic $Zn_{1-x}Fe_xAl_2O_4$ (Waerenborgh *et al.*, 1994*b*).

Substitution of Fe^{3+}(M) for Al(M) is in fact responsible for the M–O bond distance increase, Al(M)–O being definitely shorter than Fe^{3+}(M)–O (1.909 Å and 2.020 Å, respectively). This relation holds, no matter which other octahedral cations (Zn(M)–O = 2.104 Å, Mg(M)–O = 2.095 Å or Fe^{2+}(M)–O = 2.138 Å) substitute for Al(M). However, the latter substitutions are responsible for the variations in site electronic density. In any case, M site occupancy, which is dominated by Al, is less variable than that of the T site and is generally very close to 13 e^-, although in a few samples the value increases up to 14.8 e^- (SPN 116) as a consequence of Fe^{3+}(M) → Al(M) substitution and, in some samples, of the particularly high Zn(M) content (up to 0.06 apfu in SPN118).

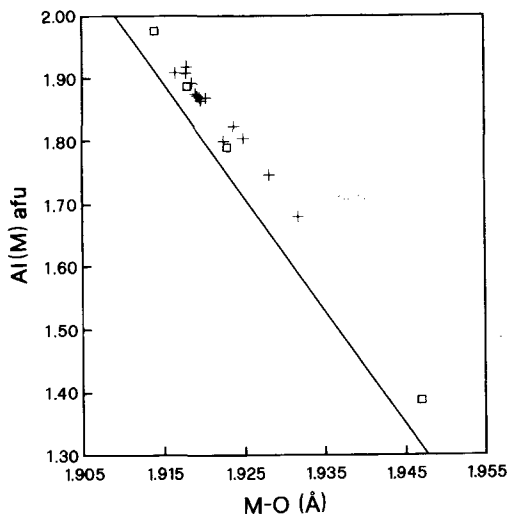

FIG. 4. Natural Zn-aluminates: Al(M) content variations *vs* M–O bond distance. Crosses: data from the present work; Open squares: synthetic $Zn(Al, Fe)_2O_4$ (Waerenborgh *et al.*, 1994*a*). Line shows calculated M–O variations with Al(M) content using bond-distance data from the present work.

Mössbauer spectral results

The iron distribution data supplied by the minimization procedure were tested by Mössbauer spectroscopy on the two samples, SPN116 and SPN118, that were available in sufficient amounts and were highly purified. The spectra show only one quadrupole split doublet due to Fe^{3+} cations. The absence of any absorption at about 2.0 mm/s is a sure indication that no Fe^{2+} is present in these crystals. The spectra can easily be fitted to just one doublet with parameters that are reasonable for Fe^{3+} in M sites. Differently from synthetic $ZnFe_2O_4$, where Fe^{3+}(M) and Fe^{3+}(T) doublets completely overlap (O'Neill, 1992), the spectrum of sample SPN116 (Fig. 5) shows evident asymmetry between the two peaks, the one at higher velocity being deeper and narrower, while that of sample SPN118 has a value which is sightly too large for the linewidth. Moreover, as the diffraction and microprobe results supported the presence of two distinct iron sites, on the basis of this suggestion and the spectral findings, an attempt was made to fit both spectra to two, strongly overlapping doublets. This approach resulted in better χ^2 values and more reliable parameters than the fitting to just one doublet, and was accepted as the most representative (Table 7). The samples are fully oxidized and contain Fe^{3+} in both M and T sites in a 3:2 (SPN118) and 4:1 (SPN116) quantitative ratio. This attribution is supported by isomer shift values characteristic of the two types of geometric coordination. The quadrupole splittings for both sites of sample SPN118 are higher than the corresponding values of sample SPN116, prob-

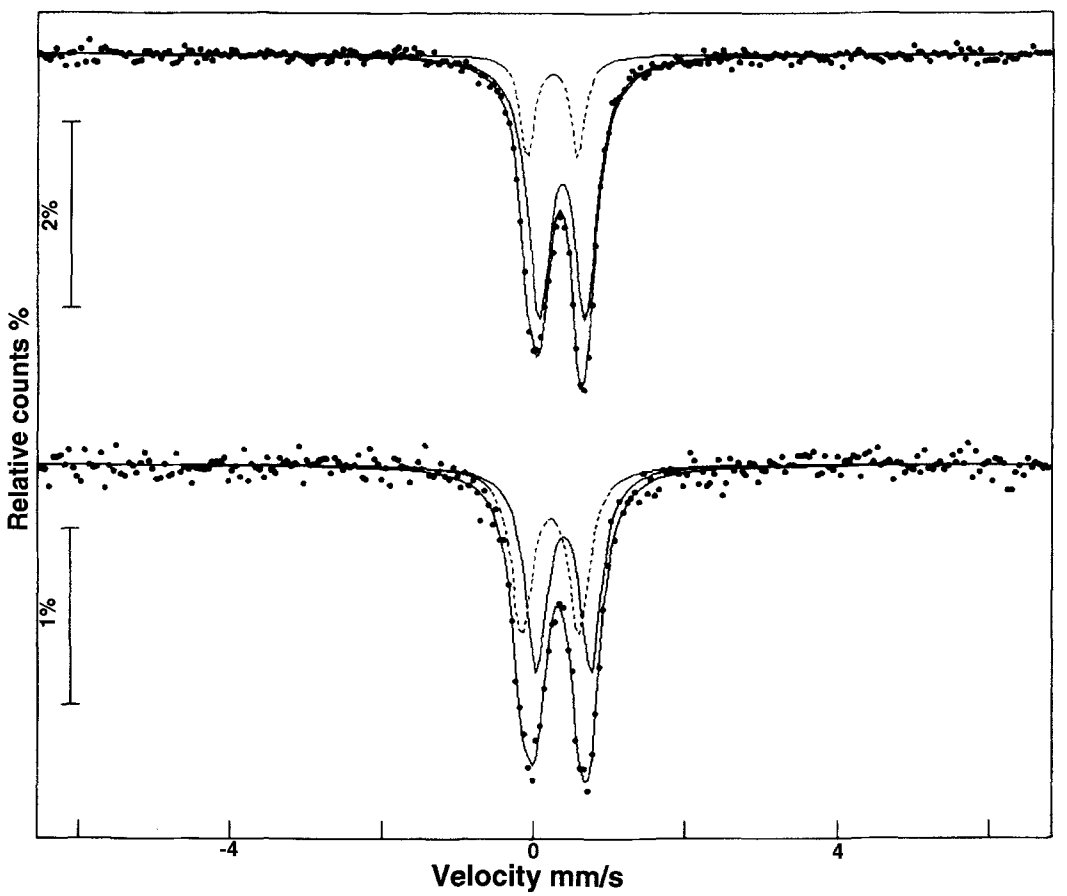

FIG. 5. Natural Zn-aluminates: Mössbauer spectra of samples SPN116 and SPN118 at room temperature.

TABLE 7. Mössbauer effect spectral parameters for SPN116 and SPN118 spinels collected at room temperature

Sample	δ mm/s	ΔE_Q mm/s	Γ mm/s	Area %	Attribution
SPN116	0.368	0.604	0.36	80	M
	0.236	0.664	0.22	20	T
SPN118	0.385	0.717	0.35	60	M
	0.214	0.748	0.32	40	T

δ: Isomer shift; ΔE_Q: Quadrupole splitting; Γ: Line full width at half height.

ably due to the presence in the former of more disordered second-coordination spheres. In each spectrum, the quadrupole splitting value of the T site is larger than that of the M site, probably because of greater disorder in the octahedral sites, which are occupied by various metal cations.

These results are very consistent with the microprobe and XRD results, no Fe^{2+} being detected in either sample (Table 4). The small residual Fe^{2+} of SPN118 is close to its standard deviation within the σ of cation distribution. The Fe^{3+} distribution obtained by the two methods is the same. The Mössbauer data give 20% Fe^{3+} in the T site for SPN116 and 40% for SPN118. These values compare well with those of 19% and 32%, obtained from the minimization procedure.

Conclusions

The main features of cation distribution in Zn-rich aluminate spinels concern evidence of Zn intracrystalline disorder. Zinc, as expected, shows a strong preference for tetrahedral coordination, but definite amounts (up to about 0.06 apfu) are also found in octahedral coordination. This is true, not only for the samples with the highest Zn content (> 0.88 apfu, samples SPN115b, 116, 117, 118, 230), but also for those with high Fe^{3+} content. Considering the quoted σ values, a satisfactory positive correlation exists between Zn(M) and Fe^{3+}(T) (Fig. 6), in agreement with the observation of the little inversion in natural franklinites (work in progress) and, at high temperatures, in synthetic Zn-ferrites (O'Neill, 1992). A negative correlation between Al(T) and Zn(M) can be seen in Fig. 6. As in Mg-Al rich spinels, Al(T) and Mg(M) are highly correlated (Fig. 7). This cation distribution agrees with the general features of that proposed by Waerenborgh *et al.* (1994*a*) for synthetic Zn spinels in the $Zn_xFe_{1-x}Al_2O_4$ system. The same authors (Waerenborgh *et al.*, 1994*b*) postulated the existence of intracrystalline disorder, although not well quantifiable, between Zn and (Al+Fe^{3+}) in synthetic $ZnFe_yAl_{2-y}O_4$ spinels, with a definitely lower contribution by Al. The latter hypothesis, of exchange between zinc and trivalent cations is only partly supported by the relation between Zn(M) and Fe^{3+}(T) observed in natural samples (Fig. 6), since Fe^{3+}(T) and Al(T) exhibit the opposite behaviour. In any case, we confirm the tendency of Zn towards crystalline

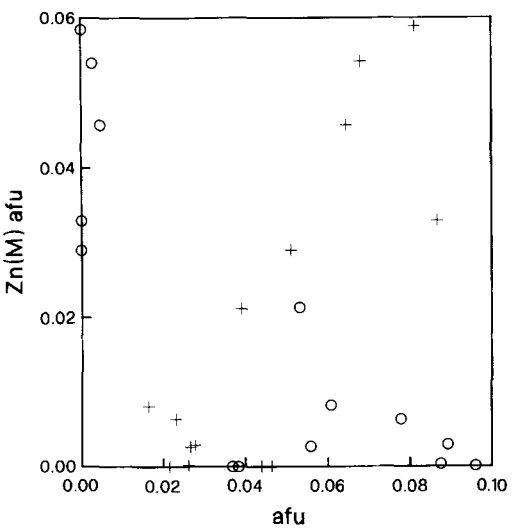

FIG. 6. Natural Zn-aluminates: Zn(M) content variations *vs* Fe^{3+}(T): crosses, and Al(T): circles.

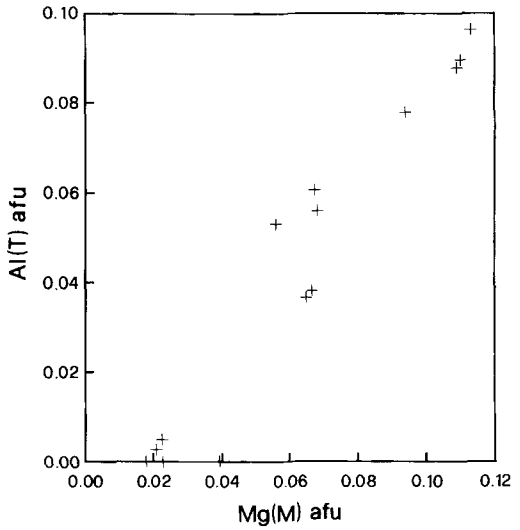

FIG. 7. Natural Zn-aluminates: Al(T) content variations *vs* Mg(M).

disorder only in the presence of appreciable amounts of trivalent iron.

The Zn(T)–O distance was optimized at 1.960 Å, shorter than the value accepted for Mg (Mg(T)–O = 1.964 Å; Della Giusta *et al.*, 1996). This is consistent both with the fact that *a* does not change relative to the main substitution of these samples, Zn → Mg (Fig. 1), and with the similarity of the *a* parameter in synthetic $MgAl_2O_4$ and $ZnAl_2O_4$, which are 8.090–8.086 Å (Grimes *et al.*, 1983; Finger *et al.*, 1986) and 8.088–8.086 Å (Fischer, 1967; Bruckmann-Benke *et al.*, 1988; Carvalho and Sclar, 1988; O'Neill and Dollase, 1994; Waerenborgh *et al.*, 1994*b*), respectively.

In the investigated spinels, Al shows its usual preference for the M site but with some 'inversion' with respect to Mg. The trend of the exchange Al(T) $\rightleftharpoons$ Mg(M) common to all samples, from high to low Zn content, can be seen in Fig. 7.

Concerning iron distribution, Fe^{2+} shows a definite preference for the T site, as already proposed by work on other natural aluminate spinels containing iron (Della Giusta *et al.*, 1996); the reported amounts of octahedral ferrous iron are very probably of the same magnitude as the corresponding error. The Fe^{2+}(T) content is linearly related to T–O bond distance (Fig. 3). The ordering of Fe^{2+} in tetrahedral sites is in good agreement with the Mössbauer investigations by Waerenborgh *et al.* (1990) on natural iron-rich gahnites of which two samples, from Falun and from Bodenmais, were compositionally similar to our samples SPN127 and SPN228. However our data, which show a general tendency towards the intracrystalline disorder of ferric iron on T and M sites in particular in SPN228, do not agree with the data of the latter authors, who showed a complete ordering of Fe^{3+} in octahedral sites.

Acknowledgements

The Director and Curator of the Museum of Mineralogy of the University of Rome "La Sapienza", Italy, are thanked for kindly making samples available. Mr. R. Carampin is thanked for his assistance during microprobe analysis at the CNR laboratory in Padova and Mrs Gabriel Walton for revision of the English text. Comments by the editor and an anonymous referee substantially improved the manuscript. This research was carried out within the scientific programs and with the financial support of the CNR (grant no. 95.04078.CT11) and a MURST grant.

References

Bruckmann-Benke, P., Chatterjee, N.D. and Aksyuk, M. (1988) Thermodynamic properties of $Zn(Al,Cr)_2O_4$ spinels at high temperatures and pressures. *Contrib. Mineral. Petrol.*, **98**, 91–6.

Carbonin, S., Russo, U. and Della Giusta, A. (1996) Cation distribution in some natural spinels from X-ray diffraction and Mössbauer spectroscopy. *Mineral. Mag.*, **60**, 335–68.

Carvalho, III, A.V. and Sclar, C.B. (1988) Experimental determination of the $ZnFe_2O_4$–$ZnAl_2O_4$ miscibility gap with application to franklinite–gahnite exolution intergrowths from the Sterling Hill mine deposit, New Jersey. *Econ. Geol.*, **83**, 1447–52.

Cooley, R.F. and Reed, J.S. (1972) Equilibrium cation distributions in $NiAl_2O_4$, $CuAl_2O_4$ and $ZnAl_2O_4$. *J. Amer. Ceram. Soc.*, **55**, 395–8.

Della Giusta, A., Princivalle, F. and Carbonin, S. (1986) Crystal chemistry of a suite of natural Cr-bearing spinels with 0.15<Cr<1.07. *Neues Jahrb. Mineral. Abh.*, **155**, 319–30.

Della Giusta, A., Carbonin, S. and Ottonello, G. (1996) Temperature-dependent disorder in a natural Mg-Al-Fe^{2+}-Fe^{3+}-spinel. *Mineral. Mag.*, **60**, 603–16.

Finger, L.W., Hazen, R.M. and Hofmeister, A.M. (1986) High-pressure crystal chemistry of spinel ($MgAl_2O_4$) and magnetite (Fe_3O_4): comparisons with silicate

spinels. *Phys. Chem. Minerals*, **13**, 215–20.

Fischer, P. (1967) Neutronenbeugungsuntersuchungen der Strukturen von $MgAl_2O_4$- und $ZnAl_2O_4$-Spinellen, in Abhängigkeit von der Vorgeschichte. *Zeits. Krist.*, **124**, 275–302.

Grimes N.W., Thompson, P. and Kay, H.F. (1983) New symmetry and structure for spinel. *Proc. Royal Soc. London*, **A386**, 333–45.

Hafner, S. (1960) Metalloxyde mit Spinellstruktur. *Schweiz. Mineral. Petrogr. Mitt.*, **40**, 208–40.

Hill, R.J., Craig, J.R. and Gibbs, G.V. (1979) Systematics of the spinel structure type. *Phys. Chem. Minerals*, **4**, 317–39.

Larson, F.K. (1970) *Crystallographic Computing*. Ed. F.R. Ahmed, Munksgaard, Copenhagen.

Larsson, L. (1995) Temperature dependent cation distribution in a natural $Mg_{0.4}Fe_{0.6}Al_2O_4$ spinel. *Neues Jahrb. Mineral., Mh.*, 173–84.

Lucchesi, S. and Della Giusta, A. (1997) Crystal chemistry of an highly disordered Mg-Al natural spinel. *Mineral. Petrol.*, in press.

Lucchesi, S., Russo, U. and Della Giusta, A. (1997) Crystal chemistry and cation distribution in some Mn-rich natural and synthetic spinels. *Eur. J. Mineral.*, **9**, 31–42.

Marshall, C.P. and Dollase, W.A. (1984) Cation arrangement in iron-zinc-chromium spinel oxides. *Amer. Mineral.*, **69**, 928–36.

Navrotsky, A. (1986) Cation-distribution energetics and heats of mixing in $MgFe_2O_4$–$MgAl_2O_4$–$ZnAl_2O_4$ and $NiAl_2O_4$–$ZnAl_2O_4$ spinels: Study by high-temperature calorimetry. *Amer. Mineral.*, **71**, 1160–9.

Nell, J., Wood, B.J. and Mason, T.O. (1989) High-temperature cation distributions in Fe_3O_4–$MgAl_2O_4$–$MgFe_2O_4$–$FeAl_2O_4$ spinels from thermopower and conductivity measurements. *Amer. Mineral.*, **74**, 339–51.

O'Neill, H.St.C. (1992) Temperature dependence of the cation distribution in zinc ferrite ($ZnFe_2O_4$) from powder XRD structural refinements. *Eur. J. Mineral.*, **4**, 571–80.

O'Neill, H.St.C. and Dollase, W.A. (1994) Crystal Structures and Cation Distributions in Simple Spinels from Powder XRD Structural Refinements: $MgCr_2O_4$, $ZnCr_2O_4$, Fe_3O_4 and the Temperature Dependence of the Cation Distribution in $ZnAl_2O_4$. *Phys. Chem. Minerals*, **20**, 541–55.

O'Neill, H.St.C. and Navrotsky, A. (1983) Simple spinel: crystallographic parameters, cation radii, lattice energies and cation distribution. *Amer. Mineral.*, **68**, 181–94.

O'Neill, H.St.C., Annersten, H. and Virgo, D. (1992) The temperature dependence of the cation distribution in magnesioferrite ($MgFe_2O_4$) from powder XRD structural refinements and Mössbauer spectroscopy. *Amer. Mineral.*, **77**, 725–40.

Princivalle, F., Della Giusta, A. and Carbonin, S. (1989) Comparative crystal chemistry of spinels from some suites of ultramafic rocks. *Mineral. Petrol.*, **40**, 117–26.

Roelofsen, J.N., Peterson, R.C. and Raudsepp, M. (1992) Structural variation in a nickel aluminate spinel ($NiAl_2O_4$). *Amer. Mineral.*, **77**, 522–8.

Saalfeld, H. (1964) Strukturdaten von Gahnit, $ZnAl_2O_4$. *Zeits. Krist.*, **120**, 476–8.

Shannon, R.D. (1976) Revised effective ionic radii and systematic studies of interatomic distances in halides and chalcogenides. *Acta Crystall.*, **A32**, 751–67.

Spry, P.G. and Scott, S.D. (1986) The stability of zincian spinels in sulfide systems and their potential as exploration guides for metamorphosed massive sulfide deposits. *Econ. Geol.*, **81**, 1446–63.

Tokonami, M. and Horiuchi, H. (1980) On the space group of spinel $MgAl_2O_4$. *Acta Cryst.*, **A36**, 122–6.

Waerenborgh, J.C., Annersten, H., Ericsson, T., Figueiredo, M.O. and Cabral, J.M.P. (1990) A Mössbauer study of natural gahnite spinels showing strongly temperature-dependent quadrupole splitting distributions. *Eur. J. Mineral.*, **2**, 267–71.

Waerenborgh, J.C., Figueiredo, M.O., Cabral, J.M.P. and Pereira, L.C.J. (1994*a*) Powder XRD Structure Refinements and ^{57}Fe Mössbauer Effect Study of Synthetic $Zn_{1-x}Fe_xAl_2O_4$ ($0<x<1$) Spinels Annealed at Different Temperatures. *Phys. Chem. Minerals*, **21**, 460–8.

Waerenborgh, J.C., Figueiredo, M.O., Cabral, J.M.P. and Pereira, L.C.J. (1994*b*) Temperature and Composition Dependence of the Cation Distribution in Synthetic $ZnFe_yAl_{2-y}O_4$ ($0 \leqslant y \leqslant 1$) Spinels. *J. Solid State Chem.*, **111**, 300–9.

Wood, B.J. and Virgo, D. (1989) Upper mantle oxidation state: Ferric iron contents of lherzolite spinels by ^{57}Fe Mössbauer spectroscopy and resultant oxygen fugacity. *Geochim. Cosmochim. Acta*, **53**, 1277–91.

Wood, B.J., Kirkpatrick, R.J. and Montez, B. (1986) Order-disorder phenomena in $MgAl_2O_4$ spinel. *Amer. Mineral.*, **71**, 999–1006.

Wu, C.C. and Mason, T.O. (1981) Thermopower measurement of cation distribution in magnetite. *J. Amer. Ceram. Soc.*, **64**, 520–2.

[*Manuscript received 3 June 1996: revised 24 April 1997*]